

## Sporadic Inclusion Body Myositis Correlates with Increased Expression and Cross-linking by Transglutaminases 1 and 2\*

(Received for publication, May 20, 1999, and in revised form, October 28, 1999)

Young-Chul Choi<sup>‡§¶</sup>, Geon Tae Park<sup>§</sup>, Tai-Seung Kim<sup>¶</sup>, Il-Nam Sunwoo<sup>‡</sup>, Peter M. Steinert<sup>§</sup>, and Soo-Youl Kim<sup>§</sup>

From the Departments of <sup>‡</sup>Neurology and <sup>¶</sup>Pathology, College of Medicine, Yonsei University, Seoul 135-270, Republic of Korea and <sup>§</sup>Laboratory of Skin Biology, NIAMS, National Institutes of Health, Bethesda, Maryland 20892-2752

**Sporadic inclusion body myositis (SIBM) is characterized by vacuolar degeneration of muscle fibers and intrafiber clusters of paired helical filaments with abnormal amyloid deposition. Because of their potential involvement in other degenerative disorders, we have examined the expression of transglutaminases (TGases) in normal and SIBM tissues. We report that at least two different enzymes, the ubiquitous TGase 2 as well as the TGase 1 enzyme, are present in muscle tissues. However, in comparison with normal tissue, the expression of TGases 1 and 2 was increased 2.5- and 4-fold in SIBM, accompanied by about a 20-fold higher total TGase activity. By immunohistochemical staining, in normal muscle, TGase 2 expression was restricted to some endomysial connective tissue elements, whereas TGase 1 and  $\beta$ -amyloid proteins were not detectable. In SIBM muscle, both TGases 1 and 2 as well as amyloid proteins were brightly expressed and co-localized in the vacuolated muscle fibers, but none of these proteins colocalized with inflammatory cell markers. Next, we isolated high molecular weight insoluble proteins from SIBM muscle tissue and showed that they were cross-linked by about 6 residues/1000 residues of the isopeptide bond. Furthermore, by amino acid sequencing of solubilized tryptic peptides, they contain amyloid and skeletal muscle proteins. Together, these findings suggest that elevated expression of TGases 1 and 2 participate in the formation of insoluble amyloid deposits in SIBM tissue and in this way may contribute to progressive and debilitating muscle disease.**

Sporadic inclusion body myositis (SIBM)<sup>1</sup> is the most common myopathy in individuals over the age of 50 years. SIBM, first described in 1971 (1), is characterized by weakness in quadriceps, triceps, and foot extensor muscle systems leading to severe muscle disability (1, 2). Although extensive studies have been reported concerning the clinical, pathological, and immunological features of the disease, its etiology and pathogenesis are not yet clear. Histology of SIBM muscle biopsy

tissues reveals abnormal muscle fibers showing rimmed vacuoles, endomysial inflammation, intracellular amyloid deposition, and abundant 15–18-nm tubulofilaments within the vacuolated muscle fibers (3). Recent studies have suggested that overexpression of the  $\beta$ -amyloid precursor protein ( $\beta$ -APP) and its abnormal deposition may induce a muscle fiber destruction (4, 5). Interestingly, in this regard there are molecular-pathologic similarities between SIBM and Alzheimer's disease (3, 6). One of the pathologic hallmarks of Alzheimer's disease is the presence of neuritic plaques consisting of  $\beta$ -amyloid peptide ( $\beta$ -A) polymers, perhaps arising from cross-linking by transglutaminase (TGase) activity (7–10).

TGases (EC 2.3.2.13) are calcium-dependent cross-linking enzymes that form an isopeptide  $N^\epsilon$ -( $\gamma$ -glutamyl)lysine bond between peptide-bound glutamine and lysine residues. In this way they stabilize intra- and extracellular proteins into macromolecular assemblies that are used for a variety of essential physiological purposes such as barrier function in epithelia, apoptosis, extracellular matrix formation, etc. (11–15). To date, a number of reports have described the presence of the ubiquitous TGase 2 enzyme in normal muscle tissues (16–19), but the role of other TGases has not been explored. In addition, there is evidence that under certain circumstances, inappropriate cross-linking by TGases might lead to pathological conditions (10, 13–15). With this in mind and the possible involvement of TGases in the pathology of neurodegenerative diseases, in this study we have investigated TGase expression in normal and SIBM muscle tissues.

### MATERIALS AND METHODS

**Human Samples**—Biopsies from vastus lateralis muscle tissue were obtained from three patients with diagnostic criteria typical of SIBM (20). Also, tissue from the same muscle site from three normal age-matched individuals without known muscle disease was obtained as byproducts of unrelated surgical procedures. All tissues were obtained with informed consent at the Severance Hospital (Seoul, Korea). Four frozen tissues (20  $\mu$ m thickness) were homogenized using a Teflon pestle with 0.1 M Tris acetate (pH 7.5), 1 mM EDTA, containing protease inhibitors (5  $\mu$ g/ml leupeptin, 5  $\mu$ g/ml aprotinin, 50  $\mu$ g/ml calpain inhibitor I, 100  $\mu$ g/ml bestatin, and 1 mM phenylmethylsulfonyl fluoride). The homogenates were used for TGase activity assays and Western blotting analysis with  $\beta$ -A antibody. To prepare total RNA for RT-PCR, control and SIBM muscle tissues were homogenized directly in a glass tube using a Teflon pestle by adding Trizol reagent (100 mg/ml) (Life Technologies, Inc.) using the manufacturer's instructions.

**Conditions for TGase Assay**—A modified TGase assay method was used to determine the enzymatic activity by measurement of the incorporation of [1,4-<sup>14</sup>C]putrescine into succinylated casein (21). The samples were mixed in a reaction mixture (0.5 ml) containing 0.1 M Tris acetate, pH 7.5, 1% succinylated casein, 1 mM EDTA, 10 mM CaCl<sub>2</sub>, 0.5% lubrol PX, 5 mM dithiothreitol, 0.15 M NaCl, and 0.5 mCi of [14C]putrescine (NEN Life Science Products; 118 Ci/mol). Following incubation at 37 °C for 1 h, the reaction was terminated by the addition of 4.5 ml of cold (4 °C) 7.5% trichloroacetic acid. The trichloroacetic acid-insoluble precipitates were collected onto GF/A glass fiber filters,

\* This work was supported by grants from Yonsei University. The costs of publication of this article were defrayed in part by the payment of page charges. This article must therefore be hereby marked "advertisement" in accordance with 18 U.S.C. Section 1734 solely to indicate this fact.

<sup>¶</sup> To whom correspondence should be addressed: Dept. of Neurology, Yongdong Severance Hospital, College of Medicine, Yonsei University, Seoul 135-270, Korea. Tel.: 82-2-3497-3320; Fax: 82-2-3462-5904; E-mail: ycchoi@yumc.yonsei.ac.kr.

<sup>1</sup> The abbreviations used are: SIBM, sporadic inclusion body myositis; TGase, transglutaminase;  $\beta$ -APP,  $\beta$ -amyloid precursor protein;  $\beta$ -A,  $\beta$ -amyloid peptide; PCR, polymerase chain reaction; RT-PCR, reverse transcriptase-PCR; HPLC, high pressure liquid chromatography; Tricine, N-[2-hydroxy-1,1-bis(hydroxymethyl)ethyl]glycine.

washed with cold 5% trichloroacetic acid, dried, and counted.

**RT-PCR Analyses**—Samples of total RNA (0.01, 0.1, or 1  $\mu$ g) were reverse transcribed at 42 °C using the first strand synthesis kit (Roche Molecular Biochemicals), and then PCR was performed for the transcripts of TGase 1, TGase 2,  $\beta$ -APPs, and  $\beta$ -actin using specific primer sets. All PCRs contained the following in 20  $\mu$ l: 1.5 mM MgCl<sub>2</sub>, 200  $\mu$ M dATP, 200  $\mu$ M dGTP, 200  $\mu$ M dTTP, 100  $\mu$ M dCTP, 10  $\mu$ M of <sup>32</sup>P-dCTP (3000 Ci/mmol), a 0.2  $\mu$ M concentration of each upstream and downstream primer, 0.5 units of *Taq* polymerase, and variable amounts of templates as required.

The specific RT-PCR primers were designed in regions of no sequence homology between each human TGase, and were confirmed with human foetkin mRNA. The PCR primer sequences are as follows: TGase 1 sense strand, 5'-GAT TGT CTT CAA GAA CCC CCT TCC C-3'; TGase 1 antisense strand, 5'-TCA TCT GAC TCC AGT CCC ATT GCT C-3'; TGase 2 sense strand, 5'-CTC GTG GAG CCA GTT ATC AAC AGC TAC-3'; TGase 2 antisense strand, 5'-TCT CGA AGT TCA CCA CCA GCT TGT G-3';  $\beta$ -actin sense strand, 5'-ATC TGG CAC ACC TTC TAC AAT GAG CTG CG-3'; and  $\beta$ -actin antisense strand, 5'-CGT CAT ACT CCT GCT TGC TGA TCC ACA TCT GC-3'. Oligonucleotide primers originally designed by Golde *et al.* (22) were used that simultaneously amplified cDNA sequence encoding  $\beta$ -APP695,  $\beta$ -APP714,  $\beta$ -APP751, and  $\beta$ -APP770. The sequence of the forward primer was 5'-CAC CAC AGA GTC TGT GGA AG-3'; the sequence of reverse primer was 5'-AGG TGT CTC GAG ATA CTT GT-3'.

The PCRs were done with conditions of one cycle of 95 °C (2 min), different numbers of cycles at 55 °C (30 s) or 65 °C (30 s), and one final cycle at 72 °C (7 min) with a Perkin-Elmer 9600 PCR machine. In order to ensure a linear relationship between the amount of PCR product and amount of total RNA, we used 25 cycles for  $\beta$ -actin and TGase 2 at 55 °C, 35 cycles for  $\beta$ -APP at 55 °C, and 35 cycles for TGase 1 at 65 °C. The higher stringency for TGase 1 was required to obtain a specific band of the correct size but suffered a much lower yield of product. The products of the PCRs were separated by gel electrophoresis on 6% TBE gels, dried, and quantitated by use of a PhosphorImager (Molecular Dynamics, Inc., Sunnyvale, CA). To confirm the cDNA sequences, the products of RT-PCRs were excised from gels and ligated into the T-vector (Novagen). After selection of colonies, DNA sequencing was performed by the Sanger method. The sequences exactly matched to the human TGase 1 or 2 cDNA sequences (23, 24).

Since no products were obtained from the other transcripts at 65 °C, direct comparisons of amounts of each transcript were not possible. Therefore, we used an established method to generate semiquantitative comparative data on the relative amounts of the various transcripts (25). This measures the relative differences in the initial numbers of transcripts between two samples by use of titration analyses of a dilution series of RNA, followed by amplification and measurement of the products. In these cases, the ratio of unlabeled to labeled dCTP used in the amplification reactions was in a large excess. As a second internal control, we constructed a standard curve using plasmid cDNAs of TGases 1 and 2 as templates and demonstrated a linear reaction rate between the amount of [<sup>32</sup>P]dCTP incorporated and a >3-order of magnitude concentration range for the amount of each transcript. Since these standard curves had the same slopes for each transcript over a 1000-fold range of the total RNA template (Fig. 2), direct comparisons of relative amounts of each specific transcript in the tissues are possible.

**Immunohistochemistry**—7- $\mu$ m transverse frozen serial sections of muscle biopsies were obtained from three SIBM patients and three age-matched normal individuals, and these were used for single and double immunofluorescence techniques. Gomori trichrome staining was also performed on adjacent sections (Figs. 3 and 4).

**Single Immunohistochemistry**—Sections were fixed in acetone at 4 °C for 10 min, rinsed in 50 mM Tris-buffered saline (pH 7.5) for 15 min, and incubated for 30 min with blocking solution containing 2% bovine serum albumin and 5% normal goat serum (for TGase 2,  $\beta$ -APP, and  $\beta$ -amyloid) or 5% horse serum (for TGase 1). The sections were then incubated overnight at 4 °C using the following antibodies: polyclonal anti-human TGase 1 made in goat (26) diluted 1:200; polyclonal anti-human TGase 2 made in rabbit (10) diluted 1:200; and monoclonal anti- $\beta$ -amyloid precursor protein and  $\beta$ -amyloid peptide (Zymed Laboratories Inc., San Francisco, CA) diluted 1:10 (27). After washing for 30 min in Tris-buffered saline, the sections were incubated with biotinylated goat anti-mouse IgG (for  $\beta$ -APP and  $\beta$ -amyloid), biotinylated goat anti-rabbit IgG (for TGase 2), or biotinylated horse anti-goat IgG (for TGase 1), followed by fluorescein isothiocyanate-avidin D (Vector Laboratory, Burlingame, CA). Slides were mounted in Vectashield (Vector) and examined with a microscope equipped with epifluorescence optics.

Controls for staining specificity were preabsorption of the primary TGase antibodies with corresponding specific protein antigens, omission of the primary antibody, or its replacement with nonimmune serum. To block nonspecific binding of antibody to Fc receptors, sections were preincubated with 1:10 diluted normal goat serum.

**Double Immunohistochemistry Using Confocal Microscopy**—This was done to examine colocalization of TGase 1 and TGase 2 antigens with  $\beta$ -APP,  $\beta$ -amyloid, and cytotoxic CD8<sup>+</sup> cells. Frozen sections were prepared as above and incubated overnight with the polyclonal antibodies against TGase 1 or TGase 2 followed by biotinylated secondary antibodies and fluorescein-conjugated avidin. The sections were then incubated with one of the following monoclonal antibodies:  $\beta$ -APP (diluted 1:10),  $\beta$ -amyloid peptide (diluted 1:10), or CD8 (dilution 1:40, Coulter Immunotech, Miami, FL). Finally, the sections were treated with trimethylrhodamine isothiocyanate-conjugated secondary antibody against mouse IgG. Similar controls to the above were used. To avoid cross-reactivity despite blocking, we confirmed the results in serial sections stained separately with each of the primary antibodies. Confocal microscopy was used for more accurate co-localization of the antigens on the surfaces of cells or muscle fibers. Images were collected as a single image, not multiply integrated, on a microscope (model LSM 410 with a 40  $\times$  1.2 NA Apochromat objective; Carl Zeiss, Thornwood, NY). The 488- and 568-nm lines of a krypton/argon laser were used for fluorescence excitation.

**Western Blotting**—Total SIBM muscle lysate (20  $\mu$ g/well) was applied on 4–20% gradient SDS gels using Tricine buffers and then transferred to polyvinylidene difluoride membranes. Western blotting was performed as established previously (26). The concentration of polyclonal anti- $\beta$ -amyloid peptide (Zymed Laboratories Inc., San Francisco, CA) was 5  $\mu$ g/ml for primary antibody and 0.1  $\mu$ g/ml for secondary antibody. The blot was then developed by enhanced chemiluminescence (Pierce). Subsequently, the identified very high molecular weight and ~70-kDa bands were cut out, eluted into SDS buffer containing Tricine, freed of SDS by ion pair extraction (28), and subjected to amino acid analysis.

**Purification of Insoluble High Molecular Weight Proteins and Measurement of Isopeptide Cross-link**—Four frozen tissue sections (20- $\mu$ m thickness) were boiled for 10 min in an extraction solution consisting of 2% (w/v) SDS and 0.1% (w/v) dithiothreitol. Insoluble proteins were sedimented by centrifugation for 5 min at 13,500  $\times$  g. They were then resuspended and extracted three more times (29, 30) and finally suspended in 0.1 M N-ethylmorpholine acetate (pH 8.3). An aliquot (10%) was used for quantitation of total protein amount by amino acid analysis. Another 30% was subjected to total enzymic digestion to release the free N<sup>ε</sup>-( $\gamma$ -glutamyl)lysine isopeptide cross-link, which was then resolved and quantitated by amino acid analysis (30). The isopeptide elutes immediately after methionine. In a related set of experiments, the isopeptide content of tissue sections was determined without prior extraction.

**Peptide Sequencing**—The remaining 50% of the insoluble proteins (~10  $\mu$ g) were digested with trypsin (Sigma; sequencing grade, about 3% by weight, 6 h at 37 °C), and peptides were resolved on a 2  $\times$  150-mm C<sub>18</sub> HPLC column (Phenomenex, nucleosil 3) using a 20–75% acetonitrile gradient and using 220- and 280-nm optics. Twenty-six peaks, all of which contained aromatic residues and thus appeared well delineated due to their higher absorption at 220 nm, were collected, dried, bound to a solid support, and analyzed in a Beckman LF3500 gas-liquid phase sequencer for 10 Edman degradation cycles. The phenylthiohydantoin-derivatized amino acid(s) released at each cycle were resolved and quantitated by HPLC (31).

## RESULTS

**Expression of TGases 1 and 2 Is Increased in SIBM Tissue**—We ascertained three SIBM patients who had developed weakness of the quadriceps muscles, atrophy and weakness of the finger flexors, and weakness of foot extensors, all features classically seen in SIBM (20). Histological and immunopathological features of muscle biopsies showed a myopathy with variation of fiber size, rimmed vacuoles, and endomysial inflammation infiltrates surrounding and invading nonnecrotic muscle fibers (data not shown, but see Fig. 3). Total TGase activity was measured in tissue extracts and found to be 16-fold higher in biopsy samples from the SIBM patients compared with normal tissues (Fig. 1).

**Elevated Levels of TGase 1 and TGase 2 mRNAs in SIBM**



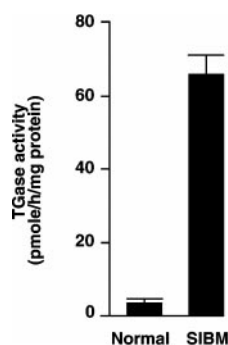


**FIG. 1. The expression of TGases 1 and 2 is increased in SIBM muscle tissues.** The TGase activities of total homogenate from SIBM tissues was about 20-fold increased over the matched normal control. These data are the averages  $\pm$  S.D. from three normal individuals as well as tissues from the three SIBM patients.

**Tissues**—To characterize the basis of this increase, we employed semiquantitative RT-PCR to estimate the relative levels of mRNAs for TGases 1 and 2 and  $\beta$ -APPs in normal and SIBM tissues. Because it was necessary to use different conditions for PCR for the transcripts of interest, direct estimates of their amounts in the tissues were not possible. Therefore, we initially determined conditions necessary to establish the linear range for the PCRs for the TGase 1 and TGase 2 transcripts using plasmid DNAs as templates by measurement of [ $^{32}$ P]dCTP incorporated during the PCR (Fig. 2A). Then we performed titration analyses with three different amounts of muscle template RNAs. We found that there was likewise a linear relationship between total RNA amounts ( $A_0$ ) and PCR ( $P$ ) product for four mRNAs of interest, and  $\beta$ -actin as an internal control (Fig. 2B). Because the amount of target mRNA is a constant proportion of the total for each dilution, the relative difference in the numbers of specific mRNA molecules is proportional to the relative differences in slopes (25), from which we could obtain semiquantitative comparative data (Fig. 2C). The data reveal several issues. First, we detected significant amounts of TGase 1 mRNA, so that this is the first report on the presence of TGase 1 in muscle tissues. Second, the amount of the  $\beta$ -actin control was very consistent for the three normal and three SIBM samples. Third, the values for the four transcripts of interest in each of the three normal or SIBM samples varied by  $<20\%$ . Notably, however, there was a 2.5-fold increase of the TGase 1 and 4-fold increase of the TGase 2 mRNA levels, respectively, in the SIBM tissues over the normal tissues. TGase 3 expression was examined but not detected in normal and SIBM tissues (data not shown). Furthermore, there was a 4-fold increase of  $\beta$ -APP-770 mRNA and a 7.5-fold increase of  $\beta$ -APP-751 mRNA in SIBM tissues. These two results are consistent with a previous observation in SIBM patients (9).

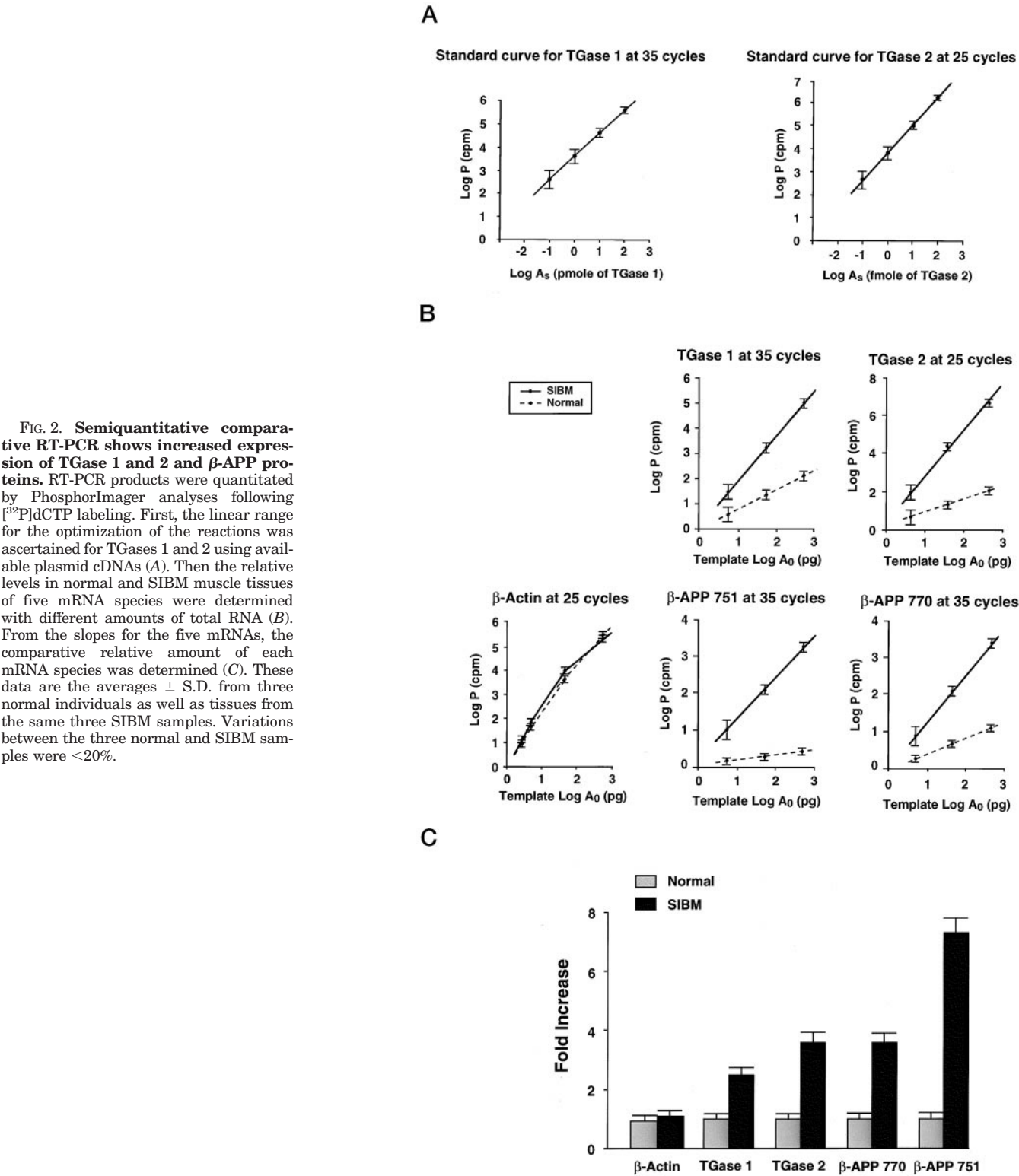
**Co-localization of Antigens for TGases 1 and 2 and  $\beta$ -Amyloid in SIBM Tissue**—In order to confirm these mRNA data, we examined the localization of TGase and amyloid antigens using immunohistochemical staining of muscle tissues from normal and SIBM individuals and using antibodies highly specific for TGase 1 (26) and TGase 2 (10) as well as for  $\beta$ -A (32) and  $\beta$ -APP (33). In normal control individuals, only TGase 2 positively stained some endomysial connective tissues (Fig. 3c), whereas staining for TGase 1 (Fig. 3b),  $\beta$ -APP (Fig. 3d), and  $\beta$ -A (not shown) antigens was very weak or negative. In order to obtain higher resolution, we used confocal microscopy. In representative sections of diseased muscle tissues from biopsies of the three patients, trichrome staining showed vacuoles and inflammation with lymphocytic infiltration (Fig. 3, e, i, m, and q), features that are typical for SIBM. The immunofluorescence

staining of TGase 1 occurred in endomysial connective tissue and was very apparent near and in the vacuoles of SIBM (Fig. 3, f and n). The staining of TGase 2 was notably increased in the endomysium connective tissue, sarcolemma at the endomysium, and the vacuoles (Fig. 3, j and r). Thus, both TGase enzymes were strongly localized in the vicinity of the vacuolar inclusions. In addition,  $\beta$ -APP (Fig. 3, g and k) and  $\beta$ -A (Fig. 3, o and s) were strongly expressed in and near the vacuoles. To examine these expression patterns in more detail, we also used double immunofluorescence staining with confocal microscopy. We consistently observed close overlap in the expression of TGase 1 and  $\beta$ -APP (Fig. 3h) or  $\beta$ -A (Fig. 3p) as well as for TGase 2 and  $\beta$ -APP (Fig. 3l) or  $\beta$ -A (Fig. 3t). Consistent with the above RT-PCR data, immunohistostaining of TGase 3 using a specific anti-human TGase 3 antibody showed no positive staining either in the normal or SIBM tissues (data not shown).

**Inflammatory Cell Infiltrates in SIBM Tissues Do Not Co-localize with TGases**—Next, we wanted to determine whether the inflammatory cells evident in the SIBM tissues contained TGases. We performed double immunofluorescence on serial sections using a CD8 T cell specific antibody (Fig. 4), since such cells account for 80%, whereas CD4-positive macrophages account for only about 20% of the invasive inflammatory cells of SIBM (33). This antibody did not stain significantly normal muscle tissue (not shown). Notably, however, the CD8-positive T cells were evident in the infiltrate of SIBM tissues, as expected (27), but did not significantly co-localize with the TGase 2 (Fig. 4c) or TGase 1 and  $\beta$ -APP antigens (data not shown). These data suggest that the invasive inflammatory cells are not a major source of the overall increased TGase presence in SIBM tissues.

**Recovery of High Molecular Weight Proteins from SIBM Tissue That Contain Isopeptide Cross-links**—Next, we investigated whether the increased expression of TGases and the large increase in TGase activity seen in SIBM contributed to the formation of cross-linked protein deposits. We performed Western blotting of total lysates of muscle biopsies using a highly specific polyclonal anti- $\beta$ -A peptide antibody (Fig. 5). Only minor immunoreactive products were seen in any of the normal muscle tissue samples. However, in all three SIBM tissue samples, positive bands of about 110 kDa were identified, which are likely to be the  $\beta$ -APP-770/751 species as previously reported (34). Interestingly, this 110-kDa band was not notably increased in the SIBM tissues as compared with normal tissues, but instead very high molecular mass proteins ( $>400$  kDa) that remained at the interface of the separation gel were prominent instead. We also observed an increase of two 60–70-kDa protein bands in the SIBM samples (Fig. 5), which, following excision from the blot and amino acid analysis after acid hydrolysis, contained only trace amounts of protein ( $<5\%$  of the high molecular weight band and insufficient for microsequencing analysis). Thus, the 60–70-kDa bands reactive with the specific antibody may be processed forms of  $\beta$ -APP.

To confirm that these high molecular weight  $\beta$ -APP-reactive proteins arise from TGase cross-linking, we employed the method established for isolation of the insoluble cornified cell envelope of the epidermis (29, 30). Muscle biopsies were exhaustively extracted by boiling with a solution containing 2.0% SDS and 0.1% dithiothreitol, and insoluble proteins were collected by centrifugation. By amino acid analyses, the insoluble proteins constituted 15% of the total protein of the SIBM tissue sections. In contrast, we could recover only trace amounts of insoluble proteins from normal tissue samples ( $<0.1\%$  of total protein). An aliquot of insoluble proteins from the SIBM tissues was then subjected to total enzymic digestion in order to release the free isopeptide cross-link. Following quantitation by



amino acid analysis (30), we found 0.6 residues of cross-link/100 residues. Interestingly, this is similar to the 1 residue/100 residues seen in the skin (30). As controls for these experiments, we determined the total amounts of cross-link in the intact tissue sections, which were 1–2 and 8–10 residues of cross-link/10,000 residues in normal and SIBM tissues, respectively. The former value, which is similar to that found in other normal tissues such as liver and brain, may represent a background degree of apoptosis (10, 14, 15). The latter value is consistent with the content of insoluble proteins recovered from

the SIBM tissues and thus indicates that the higher levels of cross-link in SIBM tissue originate from the insoluble proteins. Accordingly, these data afford the first direct report of the identification of the isopeptide cross-link in muscle tissues *in vivo*. Most significantly, the cross-link level is elevated 60-fold in the insoluble inclusion bodies of SIBM tissues.

*$\beta$ -APP Proteins and Muscle Proteins Are Present in the Insoluble Protein Fractions of SIBM Tissue*—The data of Fig. 5 are consistent with the possibility that cross-linked homo- or heteropolymers of  $\beta$ -APP proteins were generated by the in-



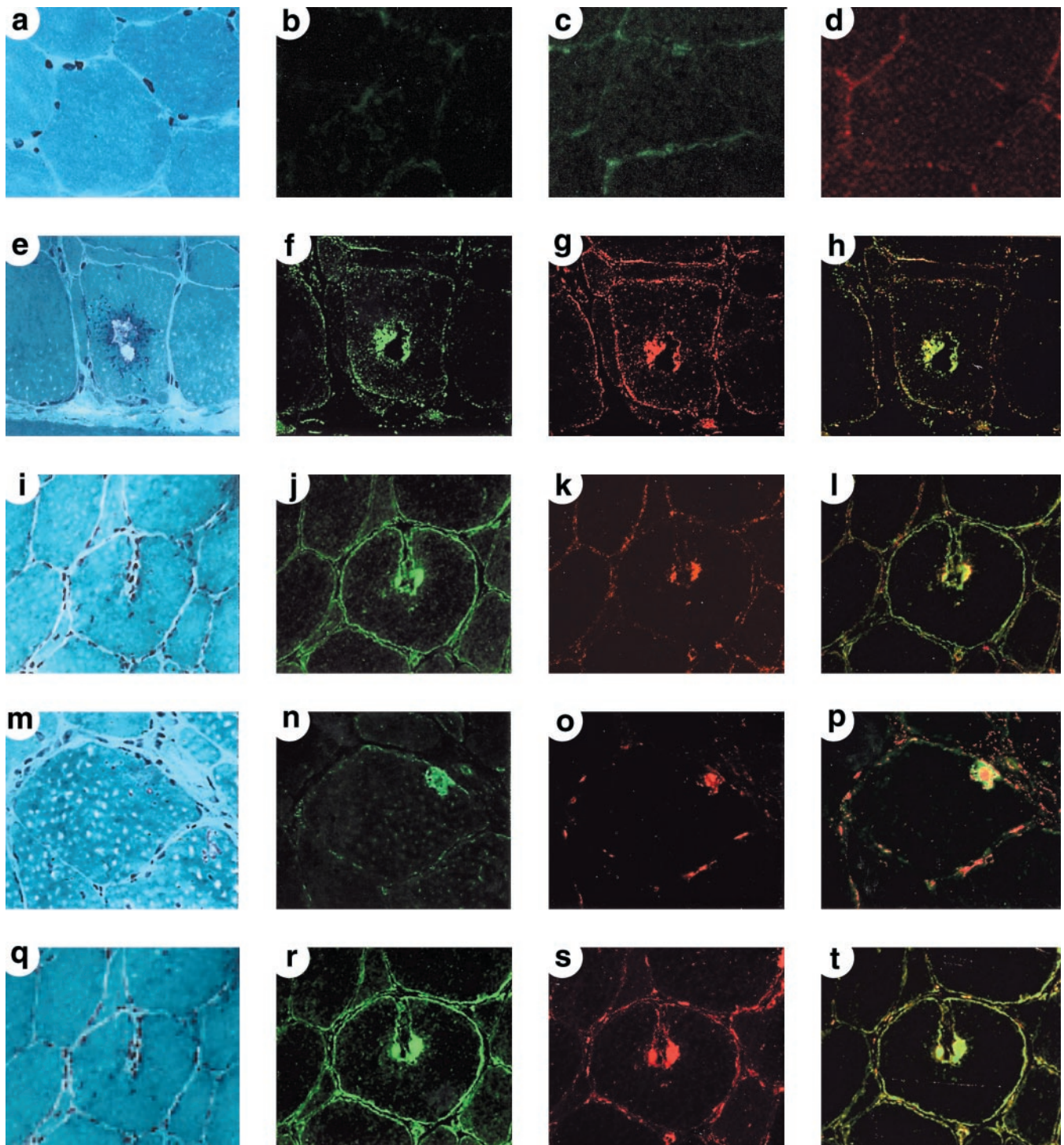


**FIG. 3. Immunohistochemical analyses reveal colocalization of TGases and  $\beta$ -amyloid proteins in SIBM muscle tissue.** The frozen sections were from normal control (*a, b, c, and d*) and SIBM (*e–t*). Gomori trichrome staining was performed in *a, e, i, m, q*. The antibodies used were anti-TGase 1 (*b, f, h, n, p*), anti-TGase 2 (*c, g, l, r, t*), anti- $\beta$ -APP (*d, g, h, k, l*), anti- $\beta$ -A (*o, p, s, t*), and double immunostaining with  $\beta$ -APP (*h, l*) or with  $\beta$ -A (*p, t*). TGase 1,  $\beta$ -APP, and  $\beta$ -A antigens were almost undetectable in normal tissue, although we detected trace amounts of mRNA by RT-PCR (Fig. 1). Both anti-TGase 1 and 2 strongly stained vacuoles in SIBM muscle along with  $\beta$ -APP (*h, p*) and  $\beta$ -A (*l, t*), and anti-TGase 2 staining also showed strong reaction in the endomysial connective tissues and sarcolemma (*j, l, r, t*).

creased TGase activity. To rigorously identify the protein content of the cross-linked high molecular weight products, a 10- $\mu$ g aliquot was subjected to digestion with trypsin, and the peptides were resolved by HPLC using a microbore column (Fig. 6). The 220-nm trace revealed numerous peaks. However, since each of these contained aromatic amino acids (280-nm trace not shown), it should be noted that the apparent sizes and shapes of the peaks are not necessarily representative of the

amounts of peptide material contained within them. In addition, the HPLC trace shows a high background of many other poorly resolved peptide peaks. A total of 26 aromatic peaks was recovered for microsequencing, and the amounts ranged from 2 to 10 pmol. Ten peptides afforded unambiguous identification from data base searches (Table I). Notably, five peptides contained sequences from either the extra- or intracellular domain of the  $\beta$ -APP protein. We also recovered several identifiable

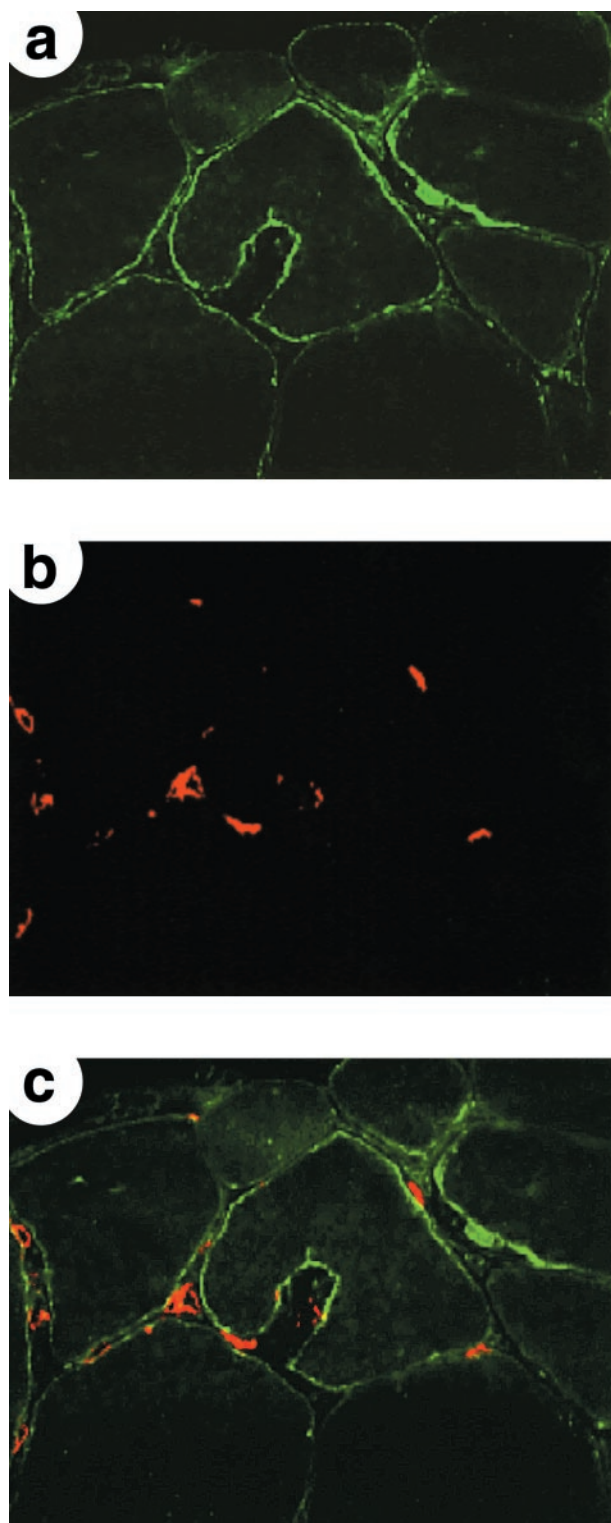


FIG. 4. Immunohistochemical analyses reveal that TGase expression does not coincide with CD8<sup>+</sup> T cell antigens in SIBM muscle tissue. We performed immunohistochemical staining on serial frozen sections from SIBM using specific antibodies: TGase 2 (a), CD8 (b), and double immunostaining of TGase 2 (green) and CD8 (red) (c). The expression of TGase 2 or TGase 1 (not shown) was not colocalized with the CD8<sup>+</sup> cells. Magnification was  $\times 400$ .

sequences from the heavy chain of skeletal myosin as well as desmin, an intermediate filament protein believed to be important for sarcomeric organization. In addition, an elevated broad poorly resolved region was found toward the end of the HPLC profile (Fig. 6), which is reminiscent of highly cross-linked

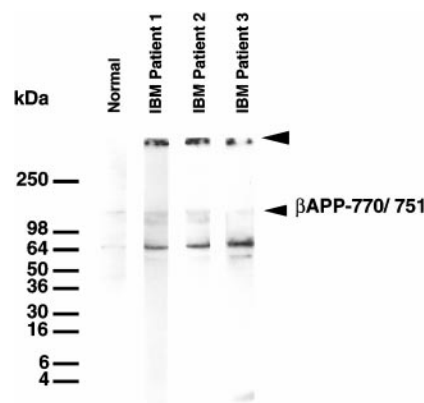


FIG. 5. The presence of insoluble cross-linked high molecular weight proteins in SIBM tissues. Western blotting with anti- $\beta$ -A antibodies revealed high molecular weight proteins at the stacking gel interface (arrowhead) as well as the expected molecular weight (arrowhead; 110 kDa). Based on amino acid analyses, the two bands in the 60–70-kDa range are probably minor (<5%) breakdown products of  $\beta$ -APP.

peptide material recovered from epidermal proteins (31, 35). Indeed, peptide peak 10 contained nearly stoichiometric sequences of both myosin and the intracellular domain of the  $\beta$ -A4 protein. Since we did not recover a glutamine residue at cycle 5 as expected for myosin, it is possible that these two proteins were in fact cross-linked together through Gln<sup>421</sup> of myosin and the downstream Lys<sup>751</sup> of the  $\beta$ -APP protein. Accordingly, these data afford direct evidence for the first time that the insoluble protein deposits in SIBM are formed *in vivo* by TGase cross-linking of amyloid proteins and intracellular muscle structural proteins.

#### DISCUSSION

**The Presence of TGases 1 and 2 in Muscle Tissues**—In this study, we have demonstrated that at least two members of the TGase enzyme family are present in muscle tissues; while the presence of the TGase 2 enzyme is well established, the present study is the first report on the involvement of the TGase 1 enzyme as well.

The TGase 1 enzyme is abundantly expressed in terminally differentiating stratified squamous epithelia, wherein it is required for barrier function by the formation of a cell envelope by cross-linking a series of defined structural proteins (14, 15, 36). Almost all of the enzyme is membrane-bound (37–39). During differentiation, some is proteolytically processed into forms with up to a 200-fold increase in specific activity (39). Thus, TGase 1 or total TGase activity levels can be increased by large amounts with only modest increases in TGase 1 expression. The properties of the TGase 2 enzyme are likewise complex. This protein serves as the G<sub>αh</sub> protein involved in signal transduction in most mammalian cells (40). However, when Ca<sup>2+</sup> concentrations rise significantly above normal intracellular levels, this ubiquitous protein becomes active in cross-linking TGase reactions (14, 15) and is largely cytosolic (11–15). Furthermore, it cannot be activated by any known process, and indeed, unlike TGase 1 or the factor XIIIa enzyme, it is inactivated when proteolyzed (10). It has been implicated in various processes such as apoptosis (41, 42), wound healing (43), and extracellular matrix stabilization (44–47). These last two observations have indicated that TGase 2 can function in the extracellular environment as well. Indeed, a recent elegant study has demonstrated that the TGase 2 enzyme binds to pericellular fibronectin through its amino-terminal  $\beta$ -sandwich domain (47). In this regard, in muscle tissues, the TGase 2 enzyme has been reported in the basal lamina and perimysial



FIG. 6. HPLC separation of tryptic peptides derived from insoluble proteins harvested from SIBM muscle tissue. Of 26 peptides collected for sequencing analyses, the identified 10 peaks yielded the recognizable sequences listed in Table I.

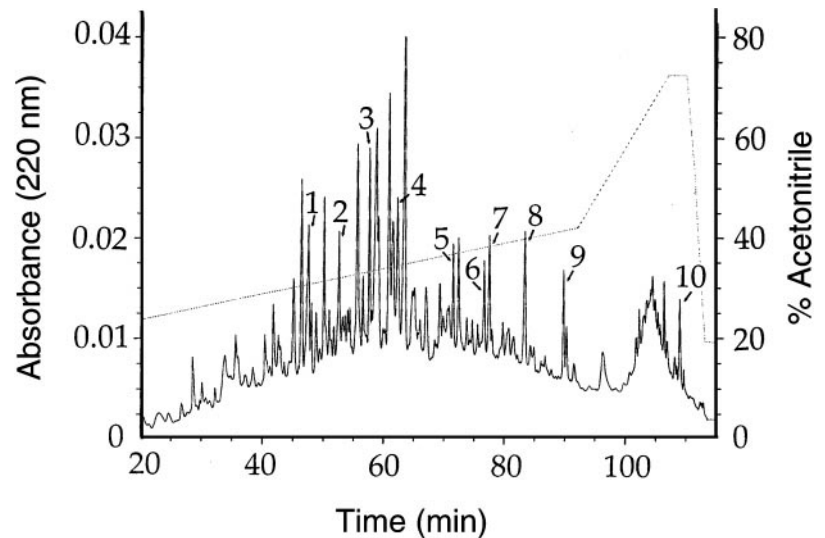


TABLE I  
Amino acid sequences and identities of peaks recovered from HPLC column

The peak numbers are as in Fig. 6. Note that most sequences shown represent only partial sequences of the tryptic peptide derived from the protein; thus, peptide 8 contains a Tyr 4 residues downstream.

Peak	Sequence	Comments
1	FANYIEK	Desmin, 119–125, 1A rod domain segment
2	YLETPGDENE	$\beta$ -APP, 378–387, extracellular domain
3	ISYGNDAI	$\beta$ -APP, 576–583, extracellular domain
4	INLPQTYSA	Desmin, 415–428, tail domain
5	AAYLTSLNSA	Myosin, 387–399, rod domain
6	LALENYITAL	$\beta$ -APP, 471–480, extracellular domain
7	QYTSIHGGV	$\beta$ -APP, 727–735, intracellular domain
8	QEAPPHIFSI	Myosin, 149–158, head domain
9	YAA-MIYTY	Myosin, 110–118, head domain
10	GQTV-QVYN	Myosin, 417–432, rod domain
	QYTSIHGG	$\beta$ -APP, 727–735, intracellular domain

connective tissue of heart muscle (13, 16). TGase 2 may contribute to the stability of the postsynaptic cholinergic system, since it was detected at neuromuscular junctions during normal neural development (17). Also, it cross-links muscle proteins in different systems (18, 19). Furthermore, one study using fetal rat myotubes reported the presence of equivalent amounts of particulate and cytosolic TGase activity (16), but detailed characterization was not performed. Likewise, we have found that 25–40% of total TGase activity in mouse skeletal muscle homogenates is present in the membrane fraction.<sup>2</sup> Based on the known properties of these two enzymes, our new data suggest that most TGase activity in normal muscle is the TGase 2 enzyme, and the significant activity present in particulate fractions is probably due to the membrane-bound TGase 1 enzyme.

**Increased Expression of TGases 1 and 2 in SIBM Disease—**Further, our new data reveal that the total levels of TGase enzyme activity are increased 20-fold in SIBM tissue. This is accompanied by a substantial increase in levels of the TGase 1 and 2 mRNAs. Although we cannot exclude the possibility in SIBM muscle tissues, to date there are no reports on widely differential mRNA stabilities for TGases 1 and 2 in epithelia (15). Thus, it is unlikely that the 4-fold increase in mRNA for TGase 2 in SIBM tissues can account for the large increase in total TGase activity. Therefore, based on the known properties of the two enzymes, we suggest that the activity increase may be due in significant part to abnormal proteolytic activation of

TGase 1 in SIBM tissue. However, we cannot exclude the possibility that other known or as yet unknown TGases may also contribute to this increase (48). Nevertheless, further detailed studies on the role and biochemistry of TGase 1 in normal and diseased muscle tissue are warranted.

Two types of data reported here point to the conclusion that this elevated TGase expression is associated with SIBM pathogenesis. First, the immunofluorescence showed a striking colocalization of abnormal deposits and/or vacuolar structures and increased TGase 1 and 2 deposition (Fig. 2). Second, we recovered significant amounts of high molecular weight proteins from SIBM tissues (~15% of total tissue protein mass) that contained about 6 residues/1000 residues of the N<sup>ε</sup>-( $\gamma$ -glutamyl)lysine isopeptide cross-link formed specifically by TGases. In contrast, we found only trace amounts of the cross-link in normal muscle tissue from the same body site. Typically proteins cross-linked to this extent *in vitro* form macromolecular aggregates (11). In natural phenomena such as apoptosis *in vivo*, these insoluble aggregates or complexes are toxic for cells (15, 41). In this way, we suggest that abnormal expression and/or activation of TGases may progressively contribute to the pathogenesis of SIBM disease.

**The Role of Increased Expression of Amyloid Proteins in SIBM—**Our RT-PCR data confirm earlier findings (9) of a severalfold increase in  $\beta$ -APP proteins in SIBM tissue (Fig. 2). Also, we found a marked apparent increase and a striking co-localization of both  $\beta$ -A and  $\beta$ -APP proteins and TGase enzymes over abnormal deposits and vacuolar inclusions in sections of SIBM tissue (Fig. 3). Furthermore, our new sequencing data revealed that at least some of the insoluble cross-linked protein aggregates recovered from SIBM tissues was derived from the  $\beta$ -APP protein (Table I). Several recent reports have demonstrated that TGase 2 can cross-link the  $\beta$ -A (49, 50) or  $\beta$ -APP (51) peptides to dimers and polymers *in vitro*. Taken together, our new data suggest that the TGase 1 enzyme, as well as TGase 2, cross-link these *in vivo* in diseased SIBM tissue.

The biological function of  $\beta$ -APP is uncertain, but it is a type I membrane protein and has been suggested to play roles in mediating cell-to-cell and cell-to-matrix interactions, maintenance of cell integrity and shape, and neuritic growth (52, 53). The  $\beta$ -APP gene produces at least three alternatively spliced transcripts encoding  $\beta$ -APP species containing 695, 751, or 770 amino acids (53). In SIBM, three epitopes of  $\beta$ -APP, amino and carboxyl termini and  $\beta$ -A, were increased and closely co-localized (54).  $\beta$ -APP mRNA (751 and/or 770) is strongly increased

<sup>2</sup> S.-Y. Kim, P. M. Steinert, and Y.-C. Choi, unpublished observations.

in muscle fibers (Ref. 9; Fig. 2). In addition, accumulation of  $\beta$ -APP and its mRNA have been demonstrated in normal neuromuscular junctions (55). Thus, it may have a specific function at the normal neuromuscular synapse.  $\beta$ -APP may also play a role in early muscle development. However, extant data suggest that its excess expression in mature adult muscle fibers may be cytotoxic (14, 56).

**Insoluble Proteins Obtained from SIBM Include Both Intracellular and Intercellular Proteins: Consequences for SIBM Pathogenesis**—Our data of Fig. 4 suggest that the increased expression of the TGase enzymes is probably not contributed by inflammatory cells that infiltrate the diseased muscle tissue (Fig. 4). However, we cannot ascertain whether the enzymes are located and functioning intra- or extracellularly (or both) because of the nature and extent of tissue degeneration of our specimens. Indeed, high resolution immunological methods at the electron microscope level, as well as availability of early disease onset tissues, may be required to provide an unambiguous answer.

Numerous proteins have been suggested as components of the inclusion bodies, based on immunological cross-reactivities (55, 57). Our new sequencing data clearly indicate that the protein deposits consist of several proteins rendered insoluble by extensive (0.6 residues/100 residues) cross-linking by the isopeptide bond. Most of the peptide peaks recovered in Fig. 6 apparently originated from the less cross-linked portions of the proteins entrapped in the insoluble macromolecular complex. These included the intracellular contractile muscle proteins myosin heavy chain and the intermediate filament structural protein desmin as well as  $\beta$ -APP sequences. This latter finding is in direct support of the earlier immunologic findings (55, 57). The recovery of contractile proteins thus points toward both intracellular as well as possible intercellular cross-linking by the increased TGase activities. Clearly, additional protein sequencing work using larger amounts of insoluble inclusion body proteins will be required to characterize the numerous minor peptide peaks seen in this study and to confirm whether they contain the many other proteins predicted to be present (55, 57). Specifically, it would be desirable to better characterize the tantalizing broad peak found late in the HPLC profile (Fig. 6), which is suggestive of tightly cross-linked peptide material (31, 35). Furthermore, sufficient inclusion body material from earlier stages of disease onset would be desirable to provide temporal information on the roles of the multiple TGases as well as disease progression.

**Conclusions**—Here we report that significantly elevated TGase 1 and 2 expression in the SIBM is correlated with markedly increased deposition of inclusion bodies containing highly cross-linked amyloid and other proteins, which may thereby contribute to the cascade of debilitating muscle disease in SIBM. Interestingly, pharmacological agents to attenuate the progression of symptoms of Alzheimer's disease also have an inhibitory effect on TGase-induced  $\beta$ -A cross-linking (58). Thus, our new findings suggest possible approaches for designing of TGase-targeted therapies in SIBM.

**Acknowledgments**—We thank Dr. Jack Folk for helpful discussions and critical review of the manuscript. We are especially grateful to Lyuben Marekov for assistance with the peptide microsequencing.

#### REFERENCES

- Yunis, E. J. & Samaha, F. J. (1971) *Lab. Invest.* **25**, 240–248
- Carpenter, S. (1996) *J. Neuropathol. Exp. Neurol.* **55**, 1105–1114
- Askanas, V. & Engel, W. K. (1988) in *Inclusion Body Myositis and Myopathies*, (Askanas, V., Serratrice, G. & Engel, W. K., eds) pp. 3–78, Cambridge University Press, Cambridge, United Kingdom
- Askanas, V., Alvarez, R. B. & Engel, W. K. (1993) *Ann. Neurol.* **34**, 551–560
- Askanas, V. & Engel, W. K. (1998) *Arch. Neurol.* **55**, 915–920
- Hardy, J. & Allsop, D. (1991) *Trends Pharmacol. Sci.* **12**, 383–388
- Masters, C. L., Simms, G., Weinman, N. A., Multhaup, G., MacDonald, B. L. & Beyreuther, K. (1985) *Proc. Natl. Acad. Sci. U. S. A.* **82**, 4245–4249
- Rasmussen, L. K., Sorensen, E. S., Petersen, T. E., Gliemann, J. & Jensen, P. H. (1994) *FEBS Lett.* **338**, 161–166
- Sarkozy, E., Askanas, V., Johnson, S. A., Engel, W. K. & Alvarez, R. B. (1993) *Neuroreport* **4**, 815–818
- Kim, S.-Y., Grant, P., Lee, J.-H., Pant, H.-C. & Steinert, P. M. (1999) *J. Biol. Chem.* **274**, 30715–30721
- Folk, J. E. (1980) *Annu. Rev. Biochem.* **49**, 517–531
- Lorand, L. & Conrad, S. M. (1984) *Mol. Cell Biochem.* **58**, 9–35
- Aeschlimann, D. & Paulsson, M. (1991) *J. Biol. Chem.* **266**, 15308–15317
- Aeschlimann, D., Mosher, D. & Paulsson, M. (1996) *Semin. Thromb. Hemostasis* **22**, 437–443
- Melino, G., Candi, E. & Steinert, P. M. (1999) *Methods Enzymol.*, **322**, in press
- Hand, D., Campoy, F. J., Clark, S., Fisher, A. & Haynes, L. W. (1993) *J. Neurochem.* **61**, 1064–1072
- Hand, D., Perry, M. J. M. & Haynes, R. H. (1993) *Int. J. Dev. Neurosci.* **11**, 709–720
- Eligula, L., Chuang, L., Phillips, M. L., Motoki, M., Seguro, K. & Muhlrad, A. (1998) *Biophys. J.* **74**, 953–963
- Nozawa, H., Mamegoshi, S. & Seki, N. (1997) *Comp. Biochem. Physiol. B Biochem. Mol. Biol.* **118**, 313–317
- Griggs, R. C., Askanas, V., DiMauro, S., Engel, A., Karpati, G., Mendell, J. R. & Rowland, L. P. (1995) *Ann. Neurol.* **38**, 705–713
- Folk, J. E. & Chung, S.-I. (1985) *Methods Enzymol.* **113**, 358–375
- Golde, T. E., Estus, S., Usiak, M., Younkin, L. H. & Younkin, S. G. (1990) *Neuron* **4**, 253–267
- Kim, I.-G., McBride, O. W., Wang, M., Kim, S.-Y., Idler, W. W. & Steinert, P. M. (1992) *J. Biol. Chem.* **267**, 7710–7717
- Gentile, V., Saydak, M., Chiocci, E. A., Akande, O., Birckbichler, P. J., Lee, K. N. & Stein, J. P. (1991) *J. Biol. Chem.* **266**, 478–483
- Singer-Sam, J., Robinson, M. O., Bellve, A. R., Simon, M. I. & Riggs, A. D. (1990) *Nucleic Acids Res.* **18**, 1255–1259
- Kim, S.-Y., Chung, S.-I., Yoneda, K. & Steinert, P. M. (1995) *J. Invest. Dermatol.* **104**, 211–217
- Engel, A. G. & Arahata, K. (1984) *Ann. Neurol.* **16**, 209–215
- Konigsberg, W. H. & Henderson, L. (1983) *Methods Enzymol.* **91**, 254–259
- Schmidt, R., Michel, S., Schroot, B. & Reichert, U. (1988) *FEBS Lett.* **229**, 193–196
- Hohl, H., Lichti, U., Turner, M. L., Roop, D. R. & Steinert, P. M. (1991) *J. Biol. Chem.* **266**, 6626–6636
- Steinert, P. M. & Marekov, L. N. (1995) *J. Biol. Chem.* **270**, 17702–17711
- Stern, R. A., Trojanowski, J. Q. & Lee, V. M. Y. (1990) *FEBS Lett.* **266**, 43–47
- Arai, H., Lee, V. W. Y., Otvos, L., Greenberg, B. D., Lowery, D. E., Sharma, S. K., Schmidt, M. L. & Trojanowski, J. Q. (1990) *Proc. Natl. Acad. Sci. U. S. A.* **87**, 2249–2253
- Di Luca, M., Pastorino, L., Bianchetti, A., Perez, J., Vignolo, L. A., Lenzi, G. L., Trabucchi, M., Cattabeni, F. & Padovani, A. (1998) *Arch. Neurol.* **55**, 1195–1200
- Candi, E., Tarcsa, E., Idler, W. W., Kartasova, T., Marekov, L. N. & Steinert, P. M. (1999) *J. Biol. Chem.* **274**, 7226–7237
- Rice, R. H. & Green, H. (1977) *Cell* **11**, 417–422
- Kim, S.-Y., Chung, S.-I., & Steinert, P. M. (1995) *J. Biol. Chem.* **270**, 18026–18035
- Steinert, P. M., Kim, S.-Y., Chung, S.-I. & Marekov, L. N. (1996) *J. Biol. Chem.* **271**, 26242–26250
- Steinert, P. M., Chung, S.-I. & Kim, S.-Y. (1996) *Biochem. Biophys. Res. Commun.* **221**, 101–106
- Nakaoka, H., Perez, D. M., Baek, K. J., Das, T., Husain, A., Misono, K., Im, M. J. & Graham, R. M. (1994) *Science* **264**, 1593–1596
- Melino, G. & Piacentini, M. (1998) *FEBS Lett.* **430**, 59–63
- Thomazy, V. A. & Davies, P. J. A. (1999) *Cell Death Differ.* **6**, 146–154
- Upchurch, H. F., Conway, E., Patterson, M. K. & Maxwell, M. D. (1991) *J. Cell Physiol.* **149**, 375–382
- Aeschlimann, D., Kaupp, O. & Paulsson, M. (1995) *J. Cell Biol.* **129**, 881–892
- Kleman, J. P., Aeschlimann, D., Paulsson, M. & van der Rest, M. (1995) *Biochemistry* **34**, 13768–13775
- Raghunath, M., Hopfner, B., Aeschlimann, D., Luthi, U., Meuli, M., Altermatt, S., Gobet, R., Bruckner-Tuderman, L. & Steinmann, B. (1996) *J. Clin. Invest.* **98**, 1174–1184
- Gaudry, C. A., Verderio, E., Aeschlimann, D., Cox, A., Smith, C. & Griffin, M. (1999) *J. Biol. Chem.* **274**, 30707–30714
- Aeschlimann, D., Koeller, M. K., Allen-Hoffmann, B. L. & Mosher, D. F. (1998) *J. Biol. Chem.* **273**, 3452–3460
- Ikkura, K., Takahata, K. & Sasaki, R. (1993) *FEBS Lett.* **326**, 109–111
- Dudek, S. M. & Johnson, G. V. W. (1994) *Brain Res.* **651**, 129–133
- Ho, G. J., Gregory, E. J., Smirnova, I. V., Zoubine, M. N. & Festoff, B. W. (1994) *FEBS Lett.* **349**, 151–154
- Selkoe, D. J. (1991) *Neuron* **6**, 487–498
- Selkoe, D. J. (1994) *Annu. Rev. Cell Biol.* **10**, 373–403
- Askanas, V., Engel, W. K. & Alvarez, R. B. (1992) *Am. J. Pathol.* **141**, 31–36
- Askanas, V., Engel, W. K. & Alvarez, R. B. (1998) *Ann. N. Y. Acad. Sci.* **841**, 28–56
- Marcon, G., Giaccone, G., Canciani, B., Cajola, L., Rossi, G., De Gioia, L., Salmona, M., Bugiani, O. & Tagliavini, F. (1999) *Am. J. Pathol.* **154**, 1001–1007
- Yang, C.-C., Askanas, V., Engel, W. K. & Alvarez, R. B. (1998) *Neurosci. Lett.* **254**, 77–80
- Zhang, W., Johnson, B. R. & Bjornsson, T. D. (1997) *Life Sci.* **60**, 2323–2332



**Sporadic Inclusion Body Myositis Correlates with Increased Expression and Cross-linking by Transglutaminases 1 and 2**

Young-Chul Choi, Geon Tae Park, Tai-Seung Kim, Il-Nam Sunwoo, Peter M. Steinert and Soo-Youl Kim

*J. Biol. Chem.* 2000, 275:8703-8710.  
doi: 10.1074/jbc.275.12.8703

---

Access the most updated version of this article at <http://www.jbc.org/content/275/12/8703>

Alerts:

- [When this article is cited](#)
- [When a correction for this article is posted](#)

[Click here](#) to choose from all of JBC's e-mail alerts

This article cites 56 references, 15 of which can be accessed free at <http://www.jbc.org/content/275/12/8703.full.html#ref-list-1>